

ISTITUTO NAZIONALE DI RICERCA METROLOGICA
Repository Istituzionale

Ultrathin random copolymer-grafted layers for block copolymer self-assembly

This is the author's submitted version of the contribution published as:

Original

Ultrathin random copolymer-grafted layers for block copolymer self-assembly / Sparnacci, Katia; Antonioli, Diego; Gianotti, Valentina; Laus, Michele; Lupi, Federico Ferrarese; Giammaria, Tommaso Jacopo; Seguini, Gabriele; Perego, Michele. - In: ACS APPLIED MATERIALS & INTERFACES. - ISSN 1944-8244. - 7:20(2015), pp. 10944-51-10951. [10.1021/acsami.5b02201]

Availability:

This version is available at: 11696/56939 since: 2018-01-30T11:03:31Z

Publisher:

American Chemical Society

Published

DOI:10.1021/acsami.5b02201

Terms of use:

This article is made available under terms and conditions as specified in the corresponding bibliographic description in the repository

Publisher copyright

American Chemical Society (ACS)

Copyright © American Chemical Society after peer review and after technical editing by the publisher. To access the final edited and published work see the DOI above.

(Article begins on next page)

1
2
3
4
5
6
7
8
9
10
11
12
13
14
15
16
17
18
19
20
21
22
23
24
25
26
27
28

On the Thermal Stability of Functional P(S-r-MMA) Random Copolymers for Nanolithographic Applications

29
30
31
32
33
34
35
36
37
38
39
40
41
42
43
44
45
46
47
48
49
50
51
52
53
54
55
56
57
58
59
60

Katia Sparnacci[§], Diego Antonioli[§], Valentina Gianotti[§], Michele Laus^{§}, Giampaolo Zuccheri[‡],
Federico Ferrarese Lupi[#], Tommaso Jacopo Giammaria[#], Gabriele Seguni[#], Monica Ceresoli^{#,‡},
and Michele Perego^{#*}*

[§] Dipartimento di Scienze e Innovazione Tecnologica (DISIT), Università del Piemonte Orientale
“A. Avogadro”, Viale T. Michel 11, 15121 Alessandria, Italy; INSTM, UdR Alessandria.

[‡] Dipartimento di Farmacia e Biotecnologie, INSTM, Centro S3, CNR-Istituto Nanoscienze, Via
Irnerio 48, Bologna 40126, Italy

[#] Laboratorio MDM, IMM-CNR, Via C. Olivetti 2, 20864 Agrate Brianza (MB), Italy

[‡]Dipartimento di Fisica, Università degli Studi di Milano, Via Celoria 16, Milano 20133 (Italy).

KEYWORDS: PS-b-PMMA, P(S-r-MMA), self assembly, rapid thermal processing (RTP),
thermal stability.

ABSTRACT: Two strategies are envisioned to improve the thermal stability of the grafted layer
and to allow the processing of the random copolymer/block copolymer system at high

1
2
3
4 temperature. From one side, a high temperature thermal treatment of a commercial α -hydroxyl
5
6 ω -TEMPO functional random copolymer, namely TR58, leads to the formation of a stabilized
7
8 layer able to induce the perpendicular orientation of a symmetric block copolymer up to
9
10 temperatures higher than 310°C. On the other side, an α -hydroxyl ω -Br functional random
11
12 copolymer, namely BrR58, with the same molar mass and composition of TR58, was prepared
13
14 by ARGET ATRP. The resulting brush layer can sustain the self assembly of the symmetric
15
16 block copolymer for processing temperature as high as 330°C. In both systems, the disruption of
17
18 the block copolymer film, deposited on the grafted random copolymer layer, occurs because of
19
20 the formation of bubbles, due to a low temperature evolution of monomers from the random
21
22 copolymer layer. The extent of the low temperature monomer evolution is higher for TR58 than
23
24 BrR58 and starts at lower temperatures. For both copolymers, the thermal treatment offsets the
25
26 low temperature monomer evolution while still maintaining surface characteristics suitable to
27
28 induce the perpendicular orientation of the block copolymers thus ultimately extending the range
29
30 of processing temperatures of the block copolymer film and consequently speeding up the self
31
32 organization process.
33
34
35
36
37
38
39

40 INTRODUCTION

41
42
43 Significant interest is currently focused on nanomanufacturing processes based on block
44
45 copolymer thin films as a viable solution to produce periodic and/or regular nanostructures at
46
47 relatively low cost^{1,2,3,4,5}. Due to their inherent self assembly propensities, a diversity of
48
49 morphologies, with periodicities spanning few to hundreds of nanometers, are available. These
50
51 nanostructured thin films, employed as nanoscale templates for pattern transfer applications,
52
53 could be exploited in several fields providing a key enabling technology for the fabrication of
54
55
56
57
58
59
60

1
2
3 nanostructured materials⁶ and/or functional features in several fields, for instance, photovoltaics,
4
5 microelectronics and nanofiltration.
6
7

8 In this regard lamellae and cylinder forming block copolymers, with nanodomains oriented
9
10 perpendicular to the underlying substrate, have several advantages in pattern transfer because of
11
12 the high aspect ratio and sharp side walls of the resulting template⁵. Consequently, the control of
13
14 the domain orientation represents a key success factor⁷. Preferential wetting of the substrate by
15
16 one of the blocks, due to the lower interfacial energy, results in parallel orientation of the
17
18 domains whereas perpendicular orientation can be achieved with non preferential interactions at
19
20 both the bottom and top interfaces. Although modified alkyl chlorosilane^{8,9} or ethylene glycol¹⁰
21
22 self-assembled monolayers (SAMs) have been used to control the wetting behavior and hence
23
24 the microdomain orientation of thin films of block copolymers, the most common strategy
25
26 involves the use of functional statistical copolymers, generally referred as random copolymer in
27
28 the literature. Even if statistical would be the proper term to identify this class of copolymers, in
29
30 the following we will refer them as random copolymers to be consistent with this consolidated
31
32 habit in the field. In this approach, the concept design underlying the formation of a neutral
33
34 surface was first described by Mansky¹¹ and consists in using end-functional poly(A-r-B)
35
36 random copolymers to generate a self-assembled monolayer chemically grafted at the substrate.
37
38 By finely tuning the composition of the random copolymer it is possible to prevent preferential
39
40 wetting and induce the perpendicular orientation of polyA-b-polyB diblock copolymers.
41
42 Although this concept has been successively extended^{12,13,14,15,16}, leading to a great variety of
43
44 functional random copolymers able to promote not only end-chain but also side-chain grafting
45
46 reactions^{17,18}, the use of functional hydroxyl terminated poly(styrene-r-methylmethacrylate)
47
48 (P(S-r-MMA)) random copolymers (RCP) is by far the most common approach to induce
49
50
51
52
53
54
55
56
57
58
59
60

1
2
3 perpendicular orientation in polystyrene-b-polymethylmethacrylate (PS-b-PMMA) block
4 copolymers (BCP). In turn, in spite of the relatively low values of the Flory-Huggins interaction
5 parameter χ which limits the resolution of domains to ca. 11 nm^{19,20}, this class of block
6 copolymers represents the current industrial standard for the implementation of novel
7 lithographic approaches based on the integration of self-assembled BCP thin films in
8 conventional photolithographic processes.
9

10
11
12
13
14
15
16
17 In the seminal study proposed by Mansky et al.¹¹, the functional P(S-r-MMA) copolymers,
18 with low molar mass and relatively narrow molar mass distribution, were prepared by nitroxide
19 mediated polymerization (NMP) using an hydroxyl (OH) functional unimolecular initiator based
20 on 2,2,6,6-tetramethylpiperidinyloxy (TEMPO) as radical controller. These P(S-r-MMA)
21 copolymers, with tailor made compositions^{21,22,23}, are terminated on the α -end with an hydroxyl
22 group and on the ω -end with the TEMPO group. The "grafting to" surface functionalization
23 consists in a thermally activated reaction of the hydroxyl group of the functional copolymer with
24 the HO-Si substrates^{24,25}. This reaction is generally performed at relatively mild temperatures (T
25 $\ll 200^\circ\text{C}$) in conventional furnaces/ovens and requires long annealing times ranging from
26 several hours to a few days¹¹. Recently, it was demonstrated that it is possible to carry out the
27 grafting process in a relatively short time²⁶ by heating the samples on a hotplate at 250°C . Then,
28 a very fast grafting procedure, involving the use of a rapid thermal processing apparatus (RTP),
29 was reported²⁷ with grafting temperatures up to 310°C at a heating rate of $20^\circ\text{C}\cdot\text{s}^{-1}$. Under these
30 conditions, the time necessary to produce the neutral layer is about 30 s. Interestingly, in the
31 same paper, the authors reported some hints of a thermally induced stabilization of the neutral
32 layer during the high temperature grafting process, suggesting the possibility to widen the
33 temperature range of the block copolymer self assembly. Although the use of solvent assisted
34
35
36
37
38
39
40
41
42
43
44
45
46
47
48
49
50
51
52
53
54
55
56
57
58
59
60

1
2
3 technologies to help the self assembly of block copolymers is widely employed^{28,29}, there are
4
5 several general and specific reasons to process block copolymers, and in particular PS-b-PMMA,
6
7 at high temperatures. In general, high temperature treatments are preferred because they offer the
8
9 possibility to considerably speed up the self assembly (SA) process and to rapidly access
10
11 thermodynamically favored morphologies, orientations, and alignments on time scales
12
13 compatible with industrial processes^{30,29}. Moreover at temperatures higher than about 225 °C, the
14
15 interfacial interactions at the free surface of PS-b-PMMA are balanced³¹, which enables a
16
17 perpendicular orientation of domains when annealed on a neutral substrate surface. In addition, a
18
19 film defectivity decrease was observed as the processing temperature increases^{32,33,34}.

20
21
22
23
24
25 The main limitation that often prevents the implementation of high temperature thermal
26
27 treatments relies on the thermal stability of the polymeric materials under investigation³⁵.
28
29 Contrary to previous claims³⁶, it was recently demonstrated³⁵ that the thermal stability in bulk
30
31 and thin film of the P(S-r-MMA) copolymers is definitely lower than that of the PS-b-PMMA
32
33 copolymers. Consequently, the range of accessible temperatures in the processing is mainly
34
35 limited by the instability of the grafted RCP layer³⁵. In principle, the BCPs exhibit a much higher
36
37 thermal stability that would allow an increase in the processing temperature and achieve the
38
39 desired level of organization in a time scale well below the requirements of the International
40
41 Technology Roadmap for Semiconductors (ITRS)³⁷.

42
43
44
45
46 In this work, we aim to identify suitable strategies to increase the thermal stability of the
47
48 random copolymer layer in order to extend the range of processing temperatures of the block
49
50 copolymer film and consequently to speed up the self organization process. For the present
51
52 investigation, a symmetric block copolymer was selected because of its higher order-disorder
53
54 transition temperature than that of an asymmetric block copolymers with similar molar mass³⁸.
55
56
57
58
59
60

1
2
3
4 This would spanning over a much broader range of processing temperatures and to extensively
5 benefit from the increased thermal stability of the random copolymer layer. Consequently,
6 random copolymers with styrene unit fraction of 58 % (Figure 1) were employed. This random
7 copolymer composition was demonstrated as very well suited²¹ in promoting the perpendicular
8 orientation of lamellar forming symmetric block copolymers.
9
10
11
12
13
14

15 Two strategies are envisioned in this paper to improve the thermal stability of the grafted layer
16 and to allow the processing of the random copolymer/block copolymer system at high
17 temperature. A commercial α -hydroxyl ω -TEMPO functional random copolymer, namely TR58,
18 is used as a reference system and a α -hydroxyl ω -Bromine functional poly(styrene-r-
19 methylmethacrylate) with the same composition of copolymer TR58, was prepared by ARGET
20 ATRP³⁹, namely BrR58, where the TEMPO moiety is substituted by a bromine atom (Figure 1).
21
22
23
24
25
26
27
28
29
30
31
32
33
34
35
36
37
38
39
40
41
42
43
44
45
46
47
48
49
50
51
52
53
54
55
56
57
58
59
60

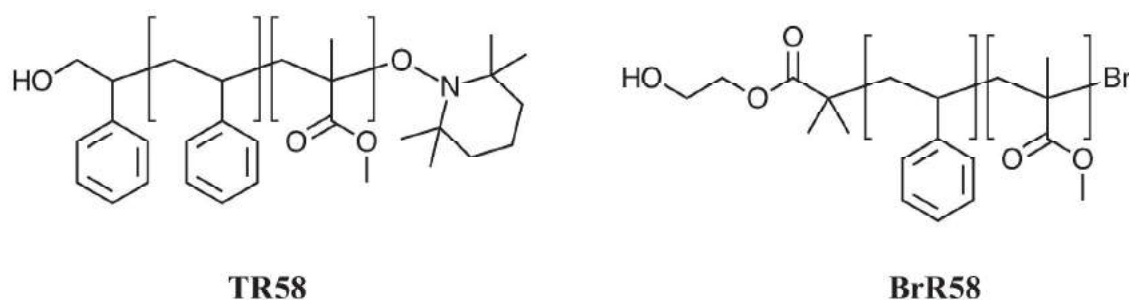


Figure 1. Structures of the α -hydroxyl functional poly(styrene-r-methylmethacrylate) (P(S-r-MMA)) random copolymers TR58 and BrR58.

EXPERIMENTAL SECTION

Materials. The α -hydroxyl ω -TEMPO functional random copolymer P(S-r-MMA) with styrene fraction of XS = 0.58 ($M_n = 11400 \text{ g}\cdot\text{mol}^{-1}$, PDI = 1.64) and the symmetric block copolymer PS-b-PMMA with styrene fraction of XS = 0.50 ($M_n = 51000 \text{ g}\cdot\text{mol}^{-1}$ and PDI = 1.06, PMMA syndiotactic rich contents >78%) were purchased from Polymer Source Inc and used as received. The RCP and the BCP were marked as TR58 and B50 where R and B stand for random and block, respectively, T for TEMPO, and the number represents the percent styrene unit. 2-hydroxyethyl(2-bromoisobutyrate) (HEBIB), tris(2-(dimethylamino)ethyl)amine (Me_6TREN), copper(II) bromide (CuBr_2), tin(II)2-ethylhexanoate ($\text{Sn}(\text{EH})_2$) and solvents were purchased from Aldrich and used as received. Styrene and methylmethacrylate were purchased from Aldrich and purified by passing through an inhibitor removal column (Aldrich) before use. The α -hydroxyl ω -Br functional P(S-r-MMA) (BrR58) was synthesized as described in the following paragraph.

ARGET ATRP copolymerization of styrene and methylmethacrylate (BrR58). The α -hydroxyl ω -Br functional random copolymer BrR58 ($M_n = 13200 \text{ g}\cdot\text{mol}^{-1}$, PDI = 1.36, XS = 0.58) was obtained by ARGET ATRP of styrene and methylmethacrylate initiated by HEBIB and catalyzed by $\text{CuBr}_2/\text{Me}_6\text{TREN}$ complex in the presence of $\text{Sn}(\text{EH})_2$ as the reducing agent³⁹.

In detail, 2.40 mg CuBr_2 (10.3 μmol) and 2.8 μl Me_6TREN (10.3 μmol) were dissolved in 6.0 ml degassed anisole, and transferred via degassed syringes to a dry Schlenk flask, purged by flushing with nitrogen. Then 8.0 ml degassed styrene (69.7 mmol), 4.0 ml degassed methylmethacrylate (37.4 mmol) and 80.0 μl HEBIB (0.55 mmol) were added and the mixture was degassed by three freeze-thaw cycles. Next, a purged solution of $\text{Sn}(\text{EH})_2$ (84.0 μmol) and

1
2
3 Me₆TREN (84.0 μmol) in degassed anisole (1.0 mL) was added and the mixture was sealed
4
5 under nitrogen. The polymerization was carried out at 90°C for 22 hours, then the reaction
6
7 mixture was cooled to room temperature and diluted with THF (5 ml). The copolymer was
8
9 precipitated into methanol, washed with methanol, and purified by precipitation from THF
10
11 solution into methanol. The copolymer composition was evaluated ¹H NMR and the styrene unit
12
13 fraction resulted XS= 0.58. The molar mass and first polydispersity index were determined by
14
15 SEC and resulted Mn = 13200 g·mol⁻¹ and PDI = 1.36, respectively.
16
17

18
19
20 *Random Copolymer Characterization.* The copolymer composition was evaluated by ¹H NMR
21
22 employing a Jeol Eclipse ECP300 spectrometer. The SEC analysis was performed on THF
23
24 solutions of the RCPs using a 590 Waters chromatograph equipped with refractive index and
25
26 ultraviolet detectors and using a column set consisting of Waters HSPgel HR3 and HR4 with a
27
28 flow rate of 0.6 mL/min. The column set was calibrated against standard PS samples.
29
30

31
32 *Substrate Preparation.* Substrates were obtained from (100) oriented Si wafers with a 50 nm
33
34 thick thermal silicon dioxide layer. Samples with surface of 1 cm² were treated with Piranha
35
36 solution (conc. H₂SO₄/30 % H₂O₂ with 3/1 vol. ratio, Warning: piranha solution reacts strongly
37
38 with organic compounds and should be handled with extreme caution) at 80°C for 40 min to
39
40 remove residual organic material and to increase the density of hydroxyl groups at the surface.
41
42 The cleaning process of the substrates was completed by rinsing in H₂O, drying in N₂ flow and
43
44 then performing an ultrasonic bath in 2-propanol.
45
46

47
48 *Random Copolymer Grafting.* Random copolymers BrR58 and TR58 (18.0 mg in solution with
49
50 2.00 mL of toluene) were spin coated on the substrates for 30 s at 4000 rpm. The samples were
51
52 then RTP thermally treated for 600 s at different temperatures from 170 to 350°C in N₂
53
54 atmosphere in order to promote the grafting reaction. A further ultrasonic bath in toluene was
55
56
57
58
59
60

1
2
3 then performed to remove the non-grafted fraction and the grafted substrate was dried under N₂
4
5 flow. To verify the effective grafting and the presence of unbounded chains, we performed
6
7 repeated washings in toluene and we observed no variation of the initial layer thickness.
8
9 Similarly, we measured the thickness of the grafted random copolymer layer after annealing the
10
11 grafted layer at 310°C for 10 min, to simulate the thermal treatment that the layer will experience
12
13 during the processing of the block copolymer spun on top of it. No variation of the random
14
15 copolymer film was detected after this treatment.
16
17

18
19
20 *Block Copolymer Deposition.* The grafted substrates were spin coated with a solution of the
21
22 B50 copolymer (16.0 mg in 2.00 mL of toluene) to obtain polymeric films with a thickness of
23
24 about 25 nm. Finally, to promote the organization of BCPs, the resulting samples were subjected
25
26 to RTP treatment at 310°C for 60 s.
27
28

29
30 *Rapid Thermal Processing Treatments.* The RTP treatments were performed in a Jipelec,
31
32 JetFirst Series system. The process consists of a three-step treatment (a heating ramp, a plateau
33
34 and a cooling ramp) in N₂ atmosphere. The temperature of the sample is constantly monitored in
35
36 real time by a thermocouple placed underneath the sample. To reach the target temperature in the
37
38 shortest possible time without over- or under- shootings, the final temperature was set about 10-
39
40 20°C higher than the target one and, as the sample temperature approaches the target
41
42 temperature, the lamp power was progressively reduced. In this way, over- or under- shootings
43
44 no higher than 1°C were obtained. In all the thermal treatments, the heating ramp was set at
45
46 18°C·s⁻¹.
47
48
49

50
51 *Film Characterization.* The thicknesses of the random and block copolymer films were
52
53 measured by a M-200U spectroscopic ellipsometer (J. A. Wollam Co. Inc.) using a Xenon lamp
54
55 at 70° incident angle. The morphological characterization of the self-assembled block-copolymer
56
57
58
59
60

1
2
3
4
5
6
7
8
9
10
11
12
13
14
15
16
17
18
19
20
21
22
23
24
25
26
27
28
29
30
31
32
33
34
35
36
37
38
39
40
41
42
43
44
45
46
47
48
49
50
51
52
53
54
55
56
57
58
59
60

films was performed by means of Scanning Electron Microscopy (SEM) in a Zeiss Supra 40 system. To improve the contrast in the SEM images the PMMA phase was selectively removed. The opening of the lamellar patterns was obtained by degrading the PMMA blocks by UV radiation exposure ($5 \text{ mW}\cdot\text{cm}^{-2}$, $\lambda = 253.7 \text{ nm}$) for 15 minutes. The samples were treated in oxygen plasma for 60 s at 40 W to remove the PMMA phase and to promote the cross-link of the PS chains. Contact angle measurements were performed using an Attension Theta Optical Tensiometer

Atomic Force Microscopy characterization of the film surface topography was performed on a Multimode NanoScope V with a J-type piezo scanner (Bruker). Imaging was performed at ambient temperature and humidity in Tapping-mode™ with NSC15/AIBS MikroMasch non-contact probes. The topography and the phase signals were acquired simultaneously.

TGA-GC-MS Copolymer Characterization. All the TGA and TGA-GC-MS analyses were performed using a Mettler TGA/SDTA 851e purged with a steady flow of inert gas at a scanning rate of $20^\circ\text{C}\cdot\text{min}^{-1}$ from room temperature to 1100°C . For bulk materials, each sample was placed in an open alumina crucible. The polymeric films on the substrate were directly placed on the thermo-balance plate. The TGA of samples TR58 and BrR58 are included as Supporting Information.

The GC-MS analysis was performed using a FINNIGAN TRACE GC-ULTRA and TRACE DSQ. The GC separation was carried out using a Phenomenex DB5-5ms capillary column (30 m, 0.25 i.d., 0.25 thickness). The injector temperature was set at 250°C in splitless mode and helium was used as carrier gas at a constant flow of $1.0 \text{ mL}\cdot\text{min}^{-1}$. The MS transfer line and the oven temperatures were set at 280 and 150°C , respectively.

1
2
3 The evolved gas from TGA was transferred to the GC-MS using the interface described in
4 detail elsewhere³⁵. The transfer lines from the TGA to the interface and from the interface to the
5 GC were set at a temperature of 200°C, the temperature of the interface was 150°C and the
6 sampling frequency was 30 s⁻¹. The sampled gas from the loop to the waste was switched after
7 10 s and the capacity of the injection loop was 2.5 mL. The MS signal was acquired in EI+ mode
8 with ionization energy of 70.0 eV and at the ion source temperature of 250 °C. The acquisition
9 was performed both in full-scan mode, in the 20–350 m·z⁻¹ range and in Single Ion Monitoring
10 (SIM) mode by acquiring the signals corresponding to styrene (S) at m·z⁻¹ = 104 and
11 methylmethacrylate (M) at m·z⁻¹ = 100.
12
13
14
15
16
17
18
19
20
21
22
23

24 *Direct Exposure Probe (DEP) analysis.* Direct mass spectrometric analysis of random
25 copolymers was performed by the DEP probe hyphenated with a quadrupolar mass spectrometer
26 (Finnigan TRACE DSQ, Thermo Electron Corporation) that permits a rapid heating of the
27 sample and the collection of the mass signals of the evolved products. Samples were deposited
28 on a filament of Rhenium, with a loop at the end, inserted in a ceramic base. A solution was
29 prepared by dissolving the relevant copolymer (2.0 mg) in dichloromethane (10.00 mL). A single
30 drop of 3 μL of this solution was deposited on the filament using a calibrated micro-syringe of
31 10 μL of volume. Then, the solvent was eliminated by heating the filament for 60 s at 50°C. The
32 filament temperature is regulated by properly adjusting the electric current flowing in the
33 filament.
34
35
36
37
38
39
40
41
42
43
44
45
46
47

48 Two distinct thermal treatments were performed as follows:

49
50 i) simple temperature scan: the sample was subjected to a conditioning step of 90 s at 25°C
51 followed by a thermal scan from 25 to 800°C with a heating rate of 1°C·s⁻¹.
52
53
54
55
56
57
58
59
60

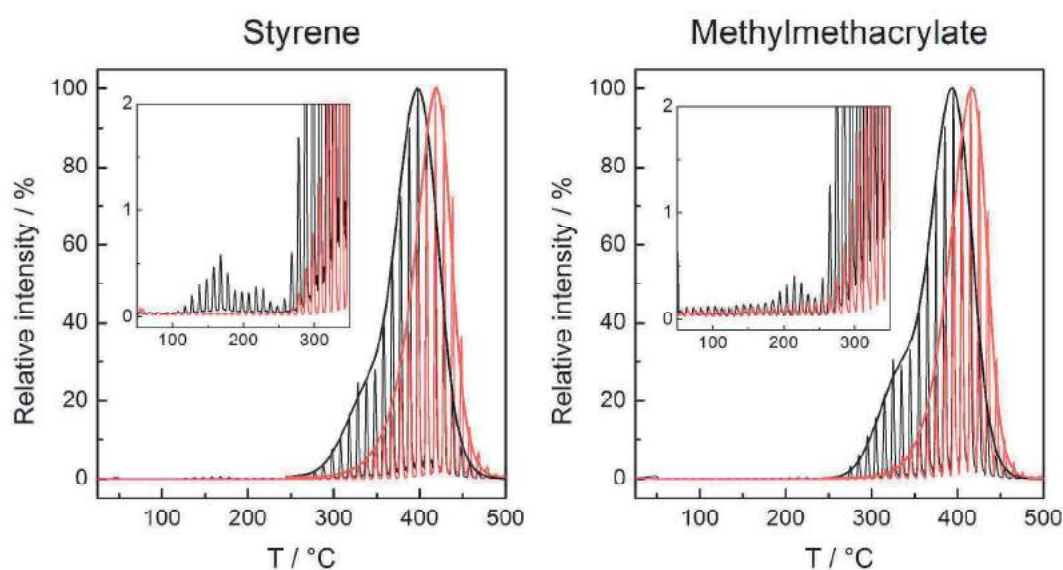
1
2
3
4
5
6
7
8
9
10
11
12
13
14
15
16
17
18
19
20
21
22
23
24
25
26
27
28
29
30
31
32
33
34
35
36
37
38
39
40
41
42
43
44
45
46
47
48
49
50
51
52
53
54
55
56
57
58
59
60

ii) RCP grafting simulation: the sample was conditioned for 90 s at 25°C, heated to the required temperature in the range between 225 to 325°C, at 20°C·s⁻¹, maintained at this temperature for a variable time period and finally cooled to room temperature by switching off the electric current in the filament. In some experiments, this treatment was followed by a simple temperature scan.

Mass spectrometric analyses were performed in EI+ mode, with an Ionization Energy of 70.0 eV and the ion source temperature of 250°C. The signal was acquired both in full scan (from 15 to 350 m·z⁻¹) and in Selected Ion Monitoring mode (SIM) by acquiring the signal corresponding to the typical m·z⁻¹ values of styrene (S) at 104 and methylnmethacrylate (M) at 100. TEMPO signal was registered at 156 m·z⁻¹ whereas Br radical was registered at 79 m·z⁻¹.

RESULTS AND DISCUSSION

RCP stability in bulk. Figure 2 illustrates the TGA-GC-MS chromatograms of both TR58 and BrR58 in bulk under nitrogen atmosphere with specific reference to the mass peaks at m·z⁻¹ 100 and 104, corresponding to methylnmethacrylate and styrene, respectively.



1
2
3
4 Figure 2. TGA-GC-MS chromatograms for the bulk thermally untreated TR58 (black curves)
5 and BrR58 (red curves) samples with specific reference to the mass peaks at $m \cdot z^{-1}$ 100 and at
6 $m \cdot z^{-1}$ 104, corresponding to methylmethacrylate and styrene, respectively.
7
8

9
10
11 The TGA heating rate was $20 \text{ }^\circ\text{C} \cdot \text{min}^{-1}$, the sampling of the evolved gas occurred every 30 s
12 and the lines, joining the gas-chromatographic peaks, mark and contour the entire loss profile. As
13 the styrene sensitivity in the mass detector is definitely higher than the one of
14 methylmethacrylate, for a direct comparison, Figure 2 reports the relative peak intensity plots
15 describing the thermal evolution of the two monomers. Apart from TEMPO molecules (not
16 included), styrene and methylmethacrylate monomers correspond to the 95% of the released
17 species. The signal intensities corresponding to dimer or trimers, even hybrid in character, are
18 extremely low. This experimental evidence suggests that the degradation of the macromolecules
19 occurs mainly through an unzipping process that leads to the progressive release of the
20 monomers forming the random copolymer.
21
22
23
24
25
26
27
28
29
30
31
32
33

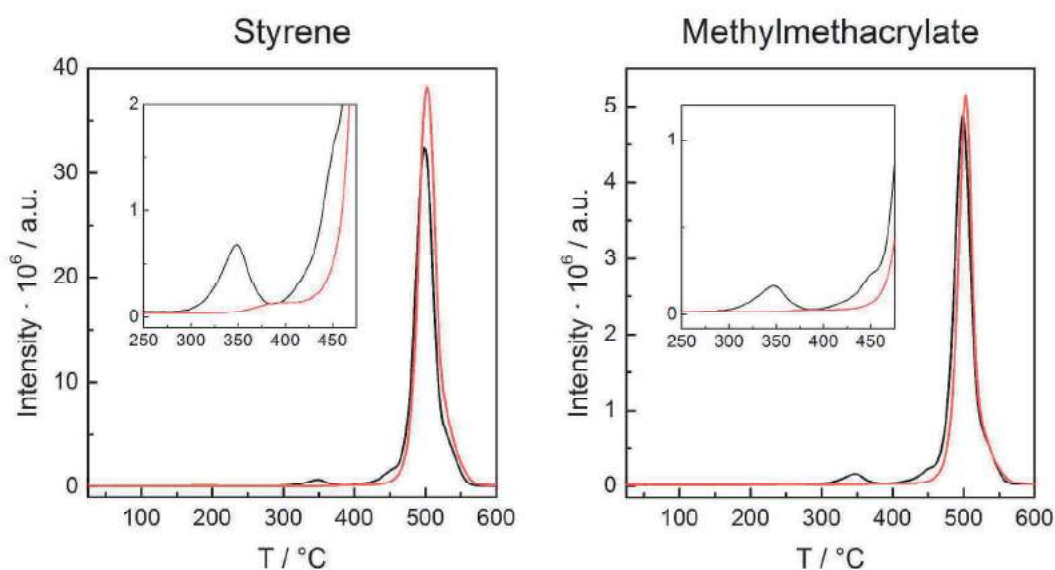
34
35 The degradation process of sample TR58 starts at about 140°C leading to the release of styrene
36 (and TEMPO molecules³⁵) and, at about ten degrees more, methylmethacrylate whereas the main
37 degradation process starts at about 240°C and ends around 460°C with the high temperature
38 volatilization profile of styrene being similar to the one of methylmethacrylate. In contrast, in the
39 degradation profile of BrR58, no low temperature losses are observed whereas, in the main
40 degradation process, the methylmethacrylate and styrene evolutions occur in a closely parallel
41 fashion, at temperatures between 320 and 460°C . These data clearly indicate that the thermal
42 stability of BrR58 is definitely higher than TR58, in agreement with existing literature
43 concerning the thermal stability of PMMA samples prepared by ATRP^{40,41} and NMP⁴². The
44 incidence of abnormal linkages, such as head-to-head and vinylidene ends is substantially
45
46
47
48
49
50
51
52
53
54
55
56
57
58
59
60

1
2
3 reduced in controlled radical polymerizations compared to conventional free radical
4 polymerizations thus increasing the thermal stability of the samples prepared by ATRP. The
5 reported TGA curves of bromine terminated PMMA are very similar to that observed in Figure 2
6 for BrR58 in which the thermal degradation occurs at about 375°C, a temperature identical to
7 that reported in the present paper for the P(S-r-MMA) copolymer prepared by ATRP. However,
8 in the case of NMP⁴², the homolytic cleavage of the C-Radical Controller, bonding occurs at
9 relatively low temperatures thus initiating the depolymerization.
10
11
12
13
14
15
16
17
18
19

20 The heating rates considered during the TGA analysis are much slower than those commonly
21 used during the RTP processing of these macromolecules. For this reason, the degradation
22 profile was also studied by MS spectrometry using the Direct Exposure Probe (DEP) tool which
23 allows^{43,44,26} heating of the sample deposited on a filament to be performed at heating rates
24 comprised between 1 and 1000°C·s⁻¹. Samples TR58 and BrR58 were subjected to the simple
25 temperature scan as described in the experimental section. The resulting monomer evolution
26 profiles, from room temperature to 600°C, are illustrated in Figure 3, and the result is
27 qualitatively similar to the one described in Figure 2 by TGA-GC-MS, although the main losses
28 are shifted to higher temperatures because of the higher heating rate (60°C·min⁻¹). This indicates
29 that the fast heating rate of the RTP technique moves the onset of the degradation of the random
30 copolymers to higher temperature values, thus potentially extending the processing window of
31 the block copolymer.
32
33
34
35
36
37
38
39
40
41
42
43
44
45
46
47

48 *Thermal stability of thin RCP films after the grafting treatment.* The effect of the grafting
49 treatment was investigated by TGA-GC-MS under dynamic conditions. The samples were
50 prepared by spinning a thin film (about 30 nm) of TR58 or BrR58 on the Si substrate.
51 Subsequently, the samples were annealed in RTP by heating the samples at 20°C·s⁻¹ from room
52
53
54
55
56
57
58
59
60

1
2
3
4 temperature to a grafting temperature of between 170 and 350°C. They were maintained at this
5
6 temperature for 10 min and then cooled down to room temperature at the maximum speed.
7
8 Finally, a washing step with toluene was performed to remove all the non-grafted material. The
9
10 relevant film thicknesses are reported in Table 1. In this way, the sample preparation procedure
11
12 exactly mimics that employed to produce the samples for the successive block copolymer
13
14 deposition.
15
16



17
18
19
20
21
22
23
24
25
26
27
28
29
30
31
32
33
34
35
36
37
38
39
40
41
42
43
44
45
46
47
48
49
50
51
52
53
54
55
56
57
58
59
60
Figure 3. DEP-MS styrene and methylmethacrylate evolution profiles for bulk thermally untreated TR58 (black curves) and BrR58 (red curves). The curves were extracted in Selected Ion Monitoring mode (SIM) by acquiring the signal corresponding to the typical $m \cdot z^{-1}$ values of styrene at 104 and methylmethacrylate at 100 with the simple thermal treatment ($1^\circ\text{C} \cdot \text{s}^{-1}$ heating rate).

The thermal stability of the grafted polymeric chains was then investigated by TGA-GC-MS analysis. As typical examples, Figure 4 reports the styrene evolution profiles for TR58 and BrR58 after RTP treatment at 230 and 330°C. The methylmethacrylate evolution parallels that of styrene and is not reported. The same Figure reports the degradation contour profile (dashed line)

1
2
3 of TR58 and BrR58 in bulk, for comparison purposes. The overall thermal degradation profile of
4
5 the two random copolymers, monitored through the evolution of the monomers, appears
6
7 translated toward higher values along the temperature scale in thin films³⁵ compared to bulk,
8
9 irrespective of the temperature of the grafting process.
10
11
12
13
14

15 Table 1. TR58 and BrR58 film thicknesses after grafting for 600 s at different temperatures.
16
17

Grafting temperature (°C)	TR58 thickness (nm)	BrR58 thickness (nm)
170	2.6	3.5
190	3.4	4.9
210	4.4	6.1
230	4.8	7.3
250	6.2	8.3
270	5.5	8.3
290	5.4	8.4
310	5.4	8.8
330	4.2	8.8
350	-	8.7

18
19
20
21
22
23
24
25
26
27
28
29
30
31
32
33
34
35
36
37
38
39
40
41
42
43
44 According to literature⁴⁵, this effect could be explained considering that, because of the small
45
46 thickness of the film, the residence time in the film of the radicals obtained from chain end
47
48 scission is too short to allow efficient radical transfer thus reducing the incidence of the radical
49
50 transfer processes. As a result, the main degradation moves toward higher temperatures.
51
52 However, when the layer thickness is between 3 and 8 nm, the degradation curves are identical,
53
54 within the experimental error⁴⁶. Consequently, a direct comparison between the degradation
55
56
57
58
59
60

profiles of the various samples can be reliably made irrespective of the minor thickness differences.

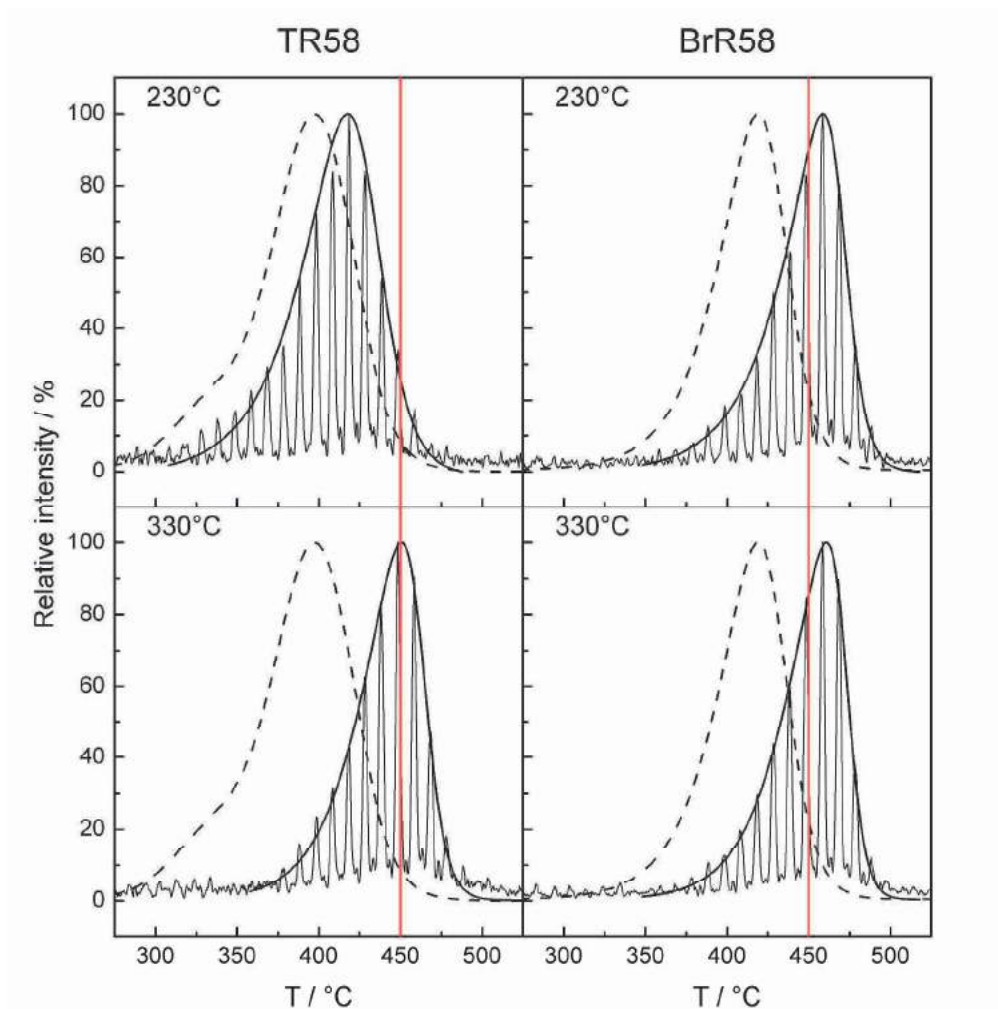


Figure 4. TGA-GC-MS analysis of styrene on TR58 and BrR58 films after the grafting process performed at 230 or 330°C. The dashed curves represent the corresponding styrene profiles for the bulk samples. The red lines at 450°C were added as a visual guide.

On the other side, the comparison between the samples annealed at 230°C and 330°C reveals quite different behavior of the two polymers. In particular, the degradation profile of the BrR58 sample is not significantly modified when increasing the grafting temperature. Conversely the

1
2
3 degradation peak of TR58 samples has remarkably shifted towards high temperature values when
4 increasing the grafting temperature from 230 to 330°C.
5
6

7
8 Figure 5 reports collectively the maximum of the degradation peak temperatures for both
9 BrR58 and TR58 samples, taken from the relevant styrene evolution profiles, as a function of the
10 grafting temperature. For the former sample, the maximum of the degradation peak displays a
11 smooth shift toward high temperatures as the grafting temperature increases, confirming our
12 previous observation. In contrast, for the latter sample, a sigmoidal trend is observed with a steep
13 increase, when the grafting process is performed at temperatures higher than 230°C. This abrupt
14 variation is followed by a smoother increase and an asymptotic stabilization at temperatures
15 higher than 290°C. This abrupt
16 increase, when the grafting process is performed at temperatures higher than 230°C. This abrupt
17 variation is followed by a smoother increase and an asymptotic stabilization at temperatures
18 higher than 290°C. This abrupt
19 variation is followed by a smoother increase and an asymptotic stabilization at temperatures
20 higher than 290°C. This abrupt
21 variation is followed by a smoother increase and an asymptotic stabilization at temperatures
22 higher than 290°C. This abrupt
23 variation is followed by a smoother increase and an asymptotic stabilization at temperatures
24 higher than 290°C. This abrupt
25 variation is followed by a smoother increase and an asymptotic stabilization at temperatures
26 higher than 290°C. This abrupt
27 variation is followed by a smoother increase and an asymptotic stabilization at temperatures
28 higher than 290°C. This abrupt
29 variation is followed by a smoother increase and an asymptotic stabilization at temperatures
30 higher than 290°C. This abrupt
31 variation is followed by a smoother increase and an asymptotic stabilization at temperatures
32 higher than 290°C. This abrupt
33 variation is followed by a smoother increase and an asymptotic stabilization at temperatures
34 higher than 290°C. This abrupt
35 variation is followed by a smoother increase and an asymptotic stabilization at temperatures
36 higher than 290°C. This abrupt
37 variation is followed by a smoother increase and an asymptotic stabilization at temperatures
38 higher than 290°C. This abrupt
39 variation is followed by a smoother increase and an asymptotic stabilization at temperatures
40 higher than 290°C. This abrupt
41 variation is followed by a smoother increase and an asymptotic stabilization at temperatures
42 higher than 290°C. This abrupt
43 variation is followed by a smoother increase and an asymptotic stabilization at temperatures
44 higher than 290°C. This abrupt
45 variation is followed by a smoother increase and an asymptotic stabilization at temperatures
46 higher than 290°C. This abrupt
47 variation is followed by a smoother increase and an asymptotic stabilization at temperatures
48 higher than 290°C. This abrupt
49 variation is followed by a smoother increase and an asymptotic stabilization at temperatures
50 higher than 290°C. This abrupt
51 variation is followed by a smoother increase and an asymptotic stabilization at temperatures
52 higher than 290°C. This abrupt
53 variation is followed by a smoother increase and an asymptotic stabilization at temperatures
54 higher than 290°C. This abrupt
55 variation is followed by a smoother increase and an asymptotic stabilization at temperatures
56 higher than 290°C. This abrupt
57 variation is followed by a smoother increase and an asymptotic stabilization at temperatures
58 higher than 290°C. This abrupt
59 variation is followed by a smoother increase and an asymptotic stabilization at temperatures
60 higher than 290°C. This abrupt

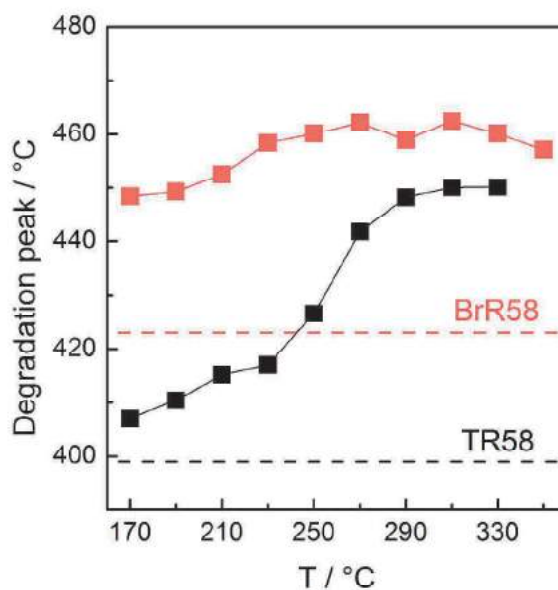


Figure 5. Maximum temperature of the degradation peak for BrR58 and TR58 in the TGA-GC-MS analysis of the styrene evolution as a function of the grafting temperature. The horizontal lines indicate the corresponding degradation temperatures for the bulk samples.

1
2
3
4 It is important to notice that the thickness of the samples subjected to the above thermal
5 treatment, even at the highest temperatures, undergoes a negligible reduction (about 0.3%). In
6 addition, the water contact angle of all these samples is not influenced by the grafting
7 temperature and results about $82 \pm 1.0^\circ$ in all cases, supporting the idea that they can be used to
8 provide a proper neutralized surface for subsequent block copolymer deposition.
9

10
11
12
13
14
15 *RCP grafting simulation by DEP-MS.* To better elucidate the effect of the thermal treatment to
16 which the polymers are subjected during the grafting process, a series of analysis was performed
17 by MS using the DEP probe, on samples deposited to the filament and subjected to the RCP
18 grafting simulation treatment as detailed in the experimental section. Both TR58 and BrR58 were
19 first heated in the DEP probe to 250 or 325°C with a heating rate of $20^\circ\text{C}\cdot\text{s}^{-1}$, maintained at this
20 temperature for different time periods between 10 and 600 s and then cooled to room
21 temperature. This treatment should simulate the thermal stress to which the random copolymers
22 are subjected during the surface grafting process. Next, the samples underwent a simple
23 temperature scan treatment to explore the effect of the thermal annealing at 250 or 325°C with
24 particular attention paid to the temperature region where the block copolymer ordering will be
25 performed (250-350°C). Figure 6 reports the DEP-MS styrene evolution of TR58 and BrR58
26 subjected to the above thermal treatments. For both copolymer samples, after the treatment at
27 250°C for 600 s, the lower temperature loss peaks are still present. In contrast, when the
28 treatment is performed at 325°C, the intensities of the styrene loss peaks progressively decrease
29 and are no longer visible after a grafting time of approximately 300 s. This result indicates that
30 the thermal degradation process, which causes a monomer loss in the low temperature region
31 which precedes the main polymer degradation, can be efficiently offset by subjecting both TR58
32 and BrR58 samples to a high temperature thermal treatment for relatively short time periods. In
33
34
35
36
37
38
39
40
41
42
43
44
45
46
47
48
49
50
51
52
53
54
55
56
57
58
59
60

1
2
3
4
5
6
7
8
9
10
11
12
13
14
15
16
17
18
19
20
21
22
23
24
25
26
27
28
29
30
31
32
33
34
35
36
37
38
39
40
41
42
43
44
45
46
47
48
49
50
51
52
53
54
55
56
57
58
59
60

addition, combining this result with the trend of the main degradation after the grafting treatments at different temperatures, illustrated in Figures 4 and 5, it may be concluded that during the thermal treatment at high temperatures, homolytic cleavage of the end groups occurs. The resulting radicals, with high local concentration, undergo bimolecular recombination or disproportionation reactions leading to the formation of more stable carbon-carbon bonds thus in turn improving the overall thermal stability of the random copolymer chains.

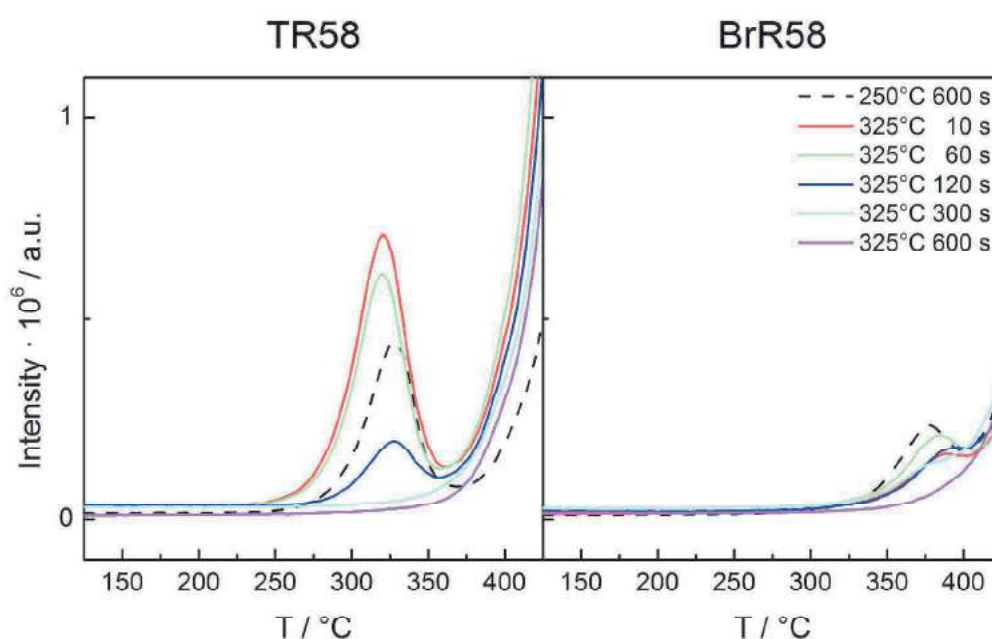
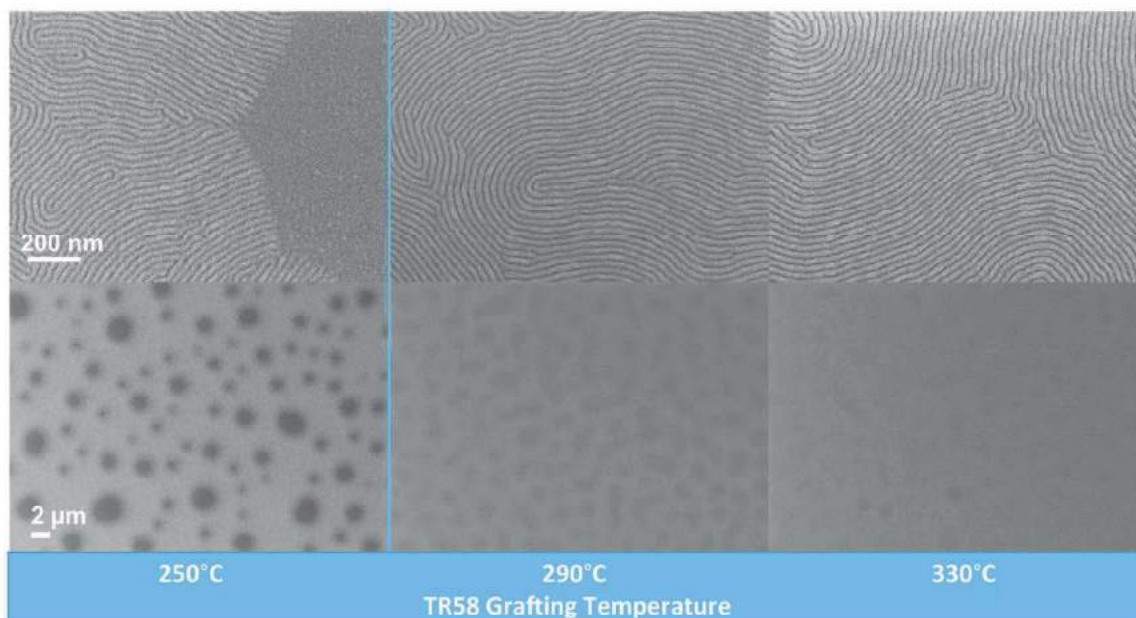


Figure 6. Styrene evolution profile for TR58 and BrR58 subjected to the following thermal treatments. The samples were first heated, with a heating rate of $20\text{ }^{\circ}\text{C}\cdot\text{s}^{-1}$, in the mass spectrometer to $250\text{ }^{\circ}\text{C}$ and maintained at this temperature for 600s (dashed line) or $325\text{ }^{\circ}\text{C}$ maintained at this temperature for different time periods and then cooled to room temperature. Finally the samples were analyzed with a heating rate of $1\text{ }^{\circ}\text{C}\cdot\text{s}^{-1}$.

Effective stability of the RCP thin film after BCP deposition. In order to test the effective stability of the random copolymer layer, a symmetric block copolymer thin film was deposited on top of the brush layer obtained by grafting the TR58 and BrR58 random copolymer thin films

1
2
3 at temperatures ranging from 250°C to 330°C for 10 min. The thickness of the BCPs films was
4 between 22 and 28 nm. The assembled stack was finally annealed at 310°C for 1 min to probe its
5 capability to withstand a severe thermal stress. As recently demonstrated, this temperature
6 represents a limiting processing value for the TR58 random copolymer when not properly
7 stabilized³⁴.
8
9

10
11 In Figure 7, the SEM plan view images of the self assembled block copolymer thin film,
12 obtained at two different magnifications, are reported as a function of the TR58 random
13 copolymer grafting temperature.
14
15
16
17
18
19
20
21

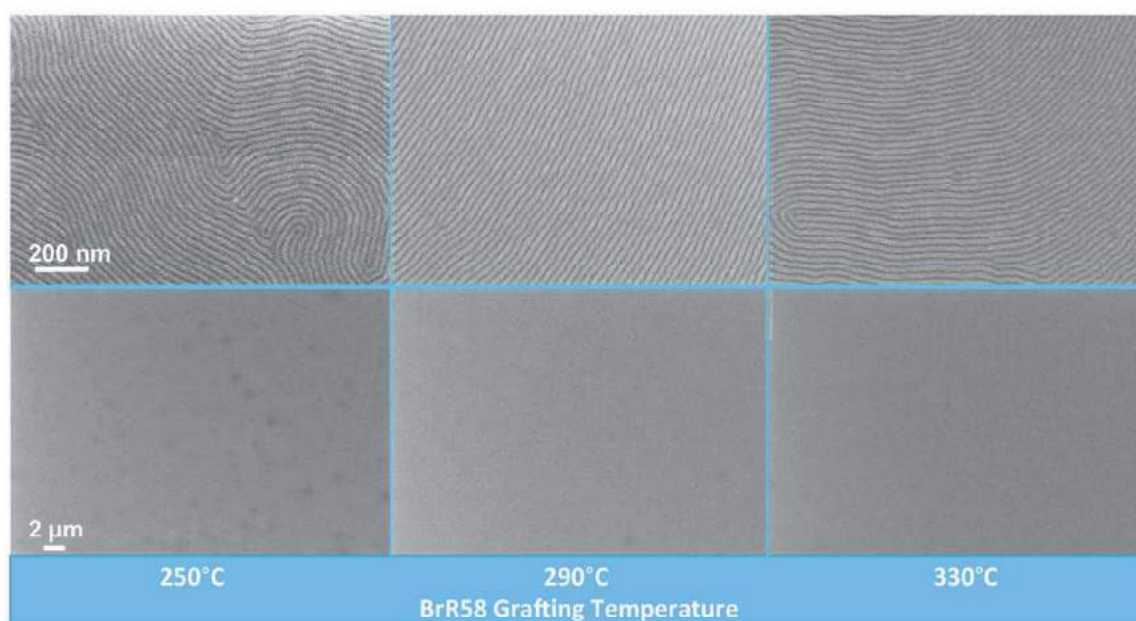


43
44 Figure 7. SEM plan view images of the self assembled block copolymer thin film as a function of
45 the TR58 random copolymer grafting temperature obtained at two different magnifications.
46
47

48
49 When looking at a small scale area, a well developed lamellar morphology can be observed in
50 all the samples irrespective of the random copolymer grafting temperature. However, the
51 observation of larger sample areas reveals the occurrence of inhomogenities in the film. In
52 particular, in the case of the random copolymer annealed at 250°C, dark spots are randomly
53
54
55
56
57
58
59
60

1
2
3 distributed over the entire film indicating the occurrence of some film degradation³⁴.
4
5 Interestingly, in the case of the random copolymer grafted at 290°C, no discontinuity in the film
6 are observed. On a large area, local variations in the contrast of the image are evident,
7 representing a warning sign of the degradation process, but no film disruption occurred. The
8 magnified SEM images indicate that the lamellar morphology is preserved even on the dark spots
9 of the film. When the sample is annealed at 330°C, the homogeneity of the film further increases
10 and only very limited modification of the contrast are visible in the large area SEM image. The
11 depicted system evolution perfectly correlates with the progressive stabilization of the TR58
12 random copolymer when annealed at high temperature as shown in Figure 5.
13
14
15
16
17
18
19
20
21
22
23
24

25 A similar SEM investigation is reported in Figure 8 for the BrR58 random copolymer.



48
49
50
51
52
53
54
55
56
57
58
59
60

Figure 8. SEM plan view images of the self assembled block copolymer thin film as a function of the BrR58 random copolymer grafting temperature obtained at two different magnifications.

The large area SEM images provide no evidence of degradation phenomena occurring in the film. The enlarged SEM images demonstrate the occurrence of phase separation in the block

1
2
3 copolymer layer and testify to the perpendicular orientation of the lamellar nanodomains with
4 respect to the substrate. The comparison between the data illustrated in Figures 7 and 8 clearly
5 indicates that the thermal stability of BrR58 is definitely higher than TR58, in perfect agreement
6 with the degradation results discussed in the previous sections.
7
8
9

10
11
12
13 The collected data indicate that, when grafting the random copolymers at 330°C, the block
14 copolymer thin films, deposited on top and thermally treated at 310°C for 60 s, are stable and
15 homogeneous with a high level of lateral order. It is worth mentioning that this processing
16 temperature of the block copolymer cannot be achieved when the random copolymer is grafted at
17 lower temperatures due to the formation of damaged areas randomly distributed on the surface of
18 the sample^{34,35}. This fact suggests that by treating the random copolymer at 330°C, it could be
19 possible to further increase the annealing temperature of the block copolymer layer and to speed
20 up the self assembly process achieving higher correlation length values.
21
22
23
24
25
26
27
28
29
30

31
32 Figure 9 compares the results obtained in the case of block copolymer thin films deposited on a
33 TR58 random copolymer brush layer grafted at 330°C for 10 min. The block copolymers were
34 annealed for 1 min at temperatures ranging from 310°C to 350°C. It is important to notice that
35 ordering of the block copolymer occurs also at this high temperature because of the weak
36 temperature dependence of the Flory-Huggins parameter for PS-b-PMMA copolymers⁴⁷. The
37 SEM plan view images highlight a progressive disruption of the polymeric film when increasing
38 the annealing temperature of the block copolymer. As it can be easily inferred from the SEM
39 plan view images reported in Figure 9, the degradation process of the polymeric stack is similar
40 to the one observed in the case of a TR58 random copolymer brush layer grafted at 250°C with
41 the formation of dark spots which gradually evolve when increasing the annealing temperature
42 and period of time³⁴.
43
44
45
46
47
48
49
50
51
52
53
54
55
56
57
58
59
60

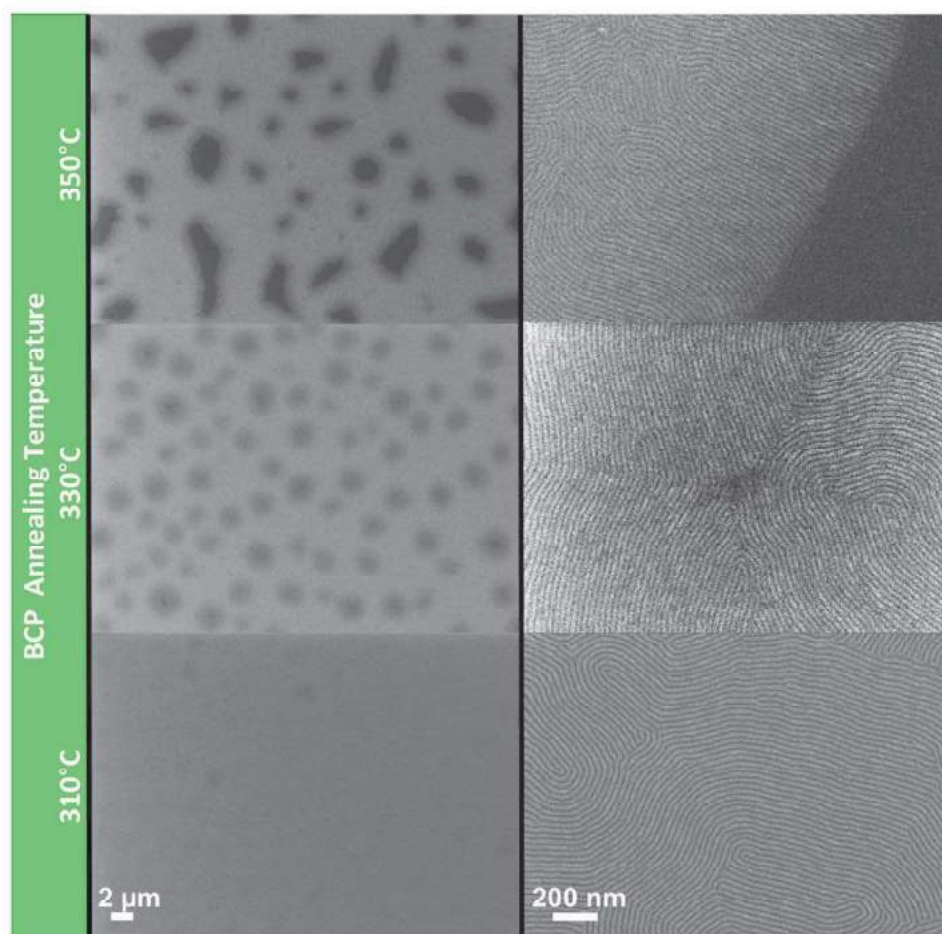
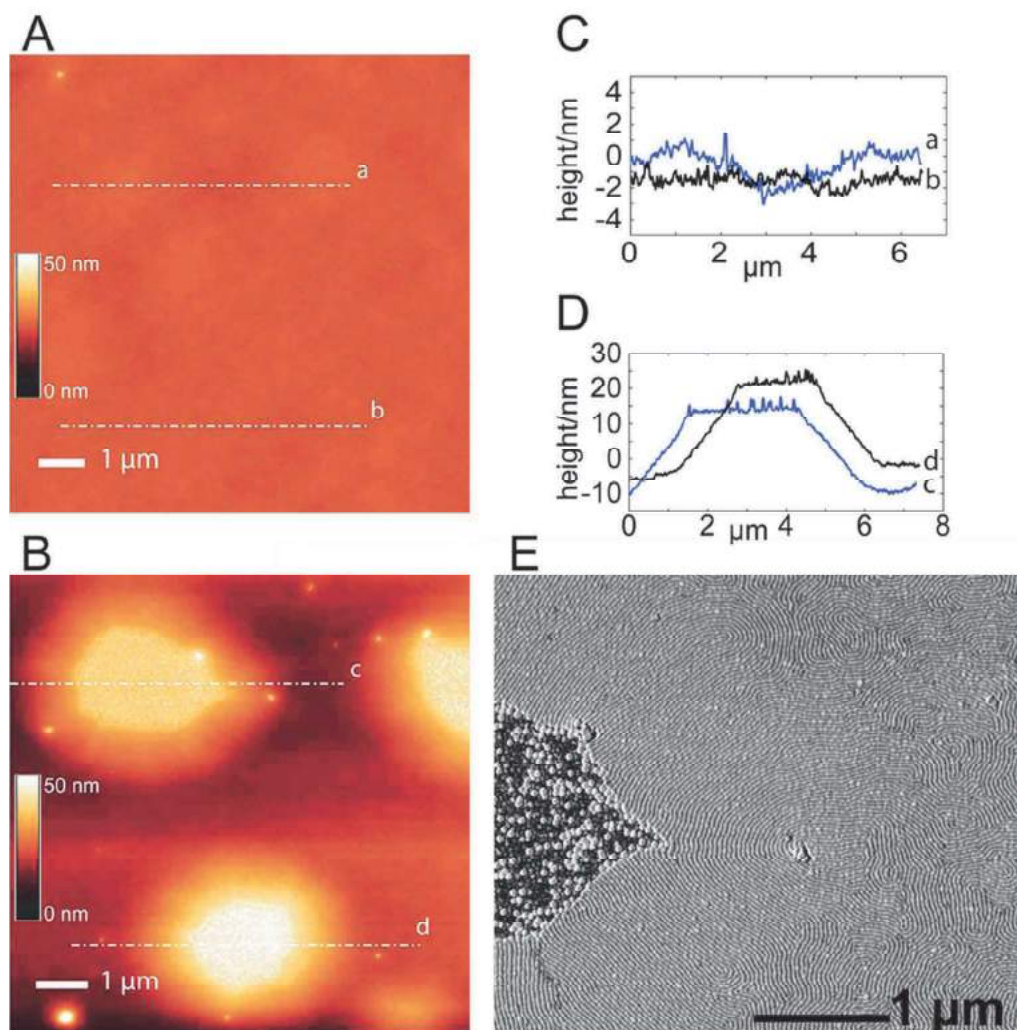


Figure 9. SEM plan view images of TR58 samples treated for 10 minutes at 330°C and then processed at different temperatures for 1 minute, once B50 was spun. The right column depicts an enlargement of a small area of the corresponding images on the left.

A detailed investigation of the degraded areas was performed by AFM analysis. The AFM images reported in Figure 10, provide information about the morphology of the block copolymer film after the high temperature treatments. Upon annealing the BCP film at 310°C, few local inhomogeneities are evident as raised point-like areas (Figure 10A). The copolymer layer starts corrugating as highlighted by the height profiles (Figure 10C) along the sections marked in panels A. The film does not break and the local arrangement of lamellae does not appear

1
2
3 significantly different in the flat areas. Annealing at 330°C produces a large number of relatively
4
5 small ruptured areas in the film with aligned lamellae arranged perpendicularly to the edges of
6
7 the rupture (data not shown).
8
9



10
11
12
13
14
15
16
17
18
19
20
21
22
23
24
25
26
27
28
29
30
31
32
33
34
35
36
37
38
39
40
41
42
43
44
45
46
47
48
49
50
51
52
53
54
55
56
57
58
59
60
Figure 10. AFM analysis of B50 film annealed at different temperatures for 1 min. The BCP film was prepared on TR58 treated at 330°C for 10 min. A) Tapping-mode topographic image showing the film after annealing at 310°C for 1 min. B) Tapping-mode topographic image of BCP film annealed at 350°C for 1 min. C) and D) traces of the height profiles along the sections marked in panels A and B, respectively. E) Detail of the AFM tapping-mode phase signal

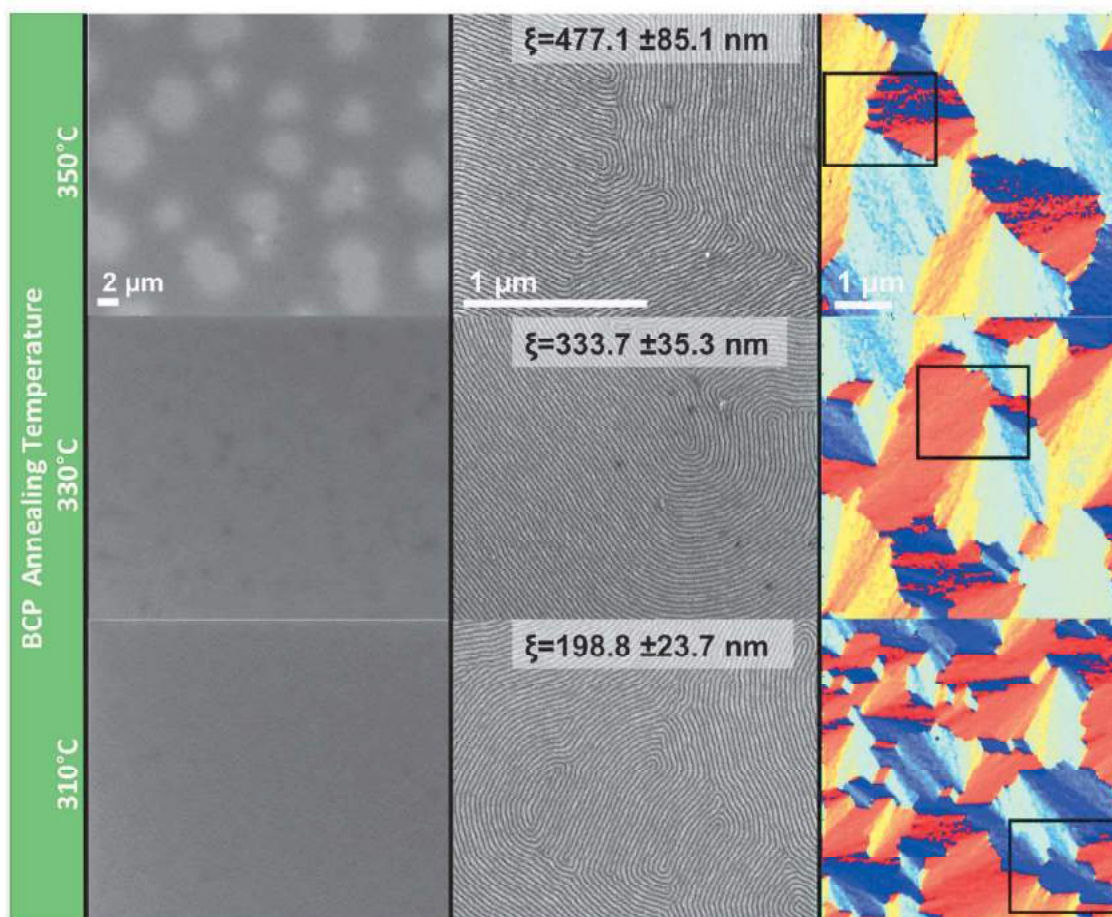
1
2
3 showing the organization of lamellae in the proximity of the ruptured area on the BCP film
4
5 annealed at 350°C.
6
7

8
9 When annealing at 350°C, ruptured areas appear larger than in the sample annealed at 330°C
10 (Figure 10B). These areas are about 25 nm higher than the nanostructured flat copolymer film
11 and present a very flat top portion (Figure 10D). Additionally, several raised point-like
12 inhomogeneities arise in the flat areas of the copolymer film. Moreover, the regions of the film
13 rising to the degraded areas display an increased level of structural order than the portions of the
14 film at a distance from these regions, often displaying lamellae arranged perpendicularly to the
15 edge of the cracks (Figure 10E).
16
17
18
19
20
21
22
23
24

25 The correlation length value measured in the block copolymer film processed at 310°C is
26 250.9 ± 30.7 nm. Nevertheless, as revealed by AFM analysis, this increase in the lateral order is
27 accompanied by a corrugation of the polymeric film that could represent a severe limitation in
28 the pattern transfer exploitation.
29
30
31
32
33
34

35 Figure 11 illustrates the results obtained for the analogous experiment performed on the BrR58
36 random copolymer brush layer thermally treated at 330°C for 10 min. In the left column in
37 Figure 11, the SEM plan view images of the block copolymer thin films annealed at 310, 330
38 and 350°C are reported. Upon raising the annealing temperature of the block copolymer layer
39 from 310 to 330°C, no significant variations in the homogeneity of the block copolymer film are
40 observed. Conversely, the SEM image of the sample annealed at 350°C shows large areas of
41 well-ordered lamellar pattern, with several bright micrometer-size spots appearing. The color
42 maps obtained from the SEM images corresponding to these samples are reported in the right
43 column of Figure 11. The images provide a direct visualization of the progressive grain
44 coarsening occurring when increasing the annealing process. The central column collects the
45
46
47
48
49
50
51
52
53
54
55
56
57
58
59
60

1
2
3
4 enlargements of the portion of the SEM images [black rectangle] corresponding to the color
5 maps reported in the right column. The correlation length values are reported in the central
6 column of Figure 11.
7
8
9



41
42
43
44
45
46
47
48
49
50
51
52
53
54
55
56
57
58
59
60

Figure 11. In the left column the SEM plan view images of block copolymer films deposited on the BrR58 brush layer (grafted at 330°C for 10 min) and subsequently processed at 310, 330 and 350° for 1 min. In the right column the color maps obtained from the SEM images corresponding to the same samples are reported. The central column reports the enlargements of a small area of the SEM images corresponding to the color maps reported in the right column.

It is clear that the increase in the annealing temperature of the block copolymer films results in a significant improvement of the lateral order, with correlation length values which are 2-3 times

1
2
3 higher than those previously reported on the same block copolymer system³⁴. Nevertheless, AFM
4 analysis of the annealed block copolymer surface, reported in Figure 12, shows that two kinds of
5 surface inhomogeneities arise after increasing the annealing temperature from 310 to 330 and
6 350°C. The BCP film annealed at 310°C shows an unperturbed flat surface with only very
7 moderate long-range corrugations (Figure 12, last row). Occasionally, raised point-like
8 inhomogeneities are found at isolated locations on the surface. Annealing the films at 330°C for
9 1 min results in a significant increase in the number of raised point-like localized
10 inhomogeneities, while the large-scale appearance of the film is still relatively flat and
11 unperturbed (Figure 12 central row), confirming the enhanced stability of the B50 film when
12 spun on the BrR58 brush layer. Annealing at 350°C for 1 min generates a number of micrometer-
13 sized film inhomogeneities (Figure 12 first row), as already evidenced by SEM analysis (Figure
14 11).

15
16
17
18
19
20
21
22
23
24
25
26
27
28
29
30
31
32 AFM images indicate that the nature of these inhomogeneities is significantly different from
33 the film ruptures observed in the case of the B50 BCP film spun on TB58 brush layer. Upon
34 annealing at 350°C, the B50 film deposited on the BrR58 brush layer exhibits large concavities
35 without any evidence of film rupture. The lamellar nanoscale structure is preserved and no
36 significant discontinuities in the lamellar organization are observed along the concavities. Even
37 the film annealed at 350°C presents small raised point-like film inhomogeneities, albeit in an
38 apparently smaller number than on the film annealed at 330°C.
39
40
41
42
43
44
45
46
47
48
49
50
51
52
53
54
55
56
57
58
59
60

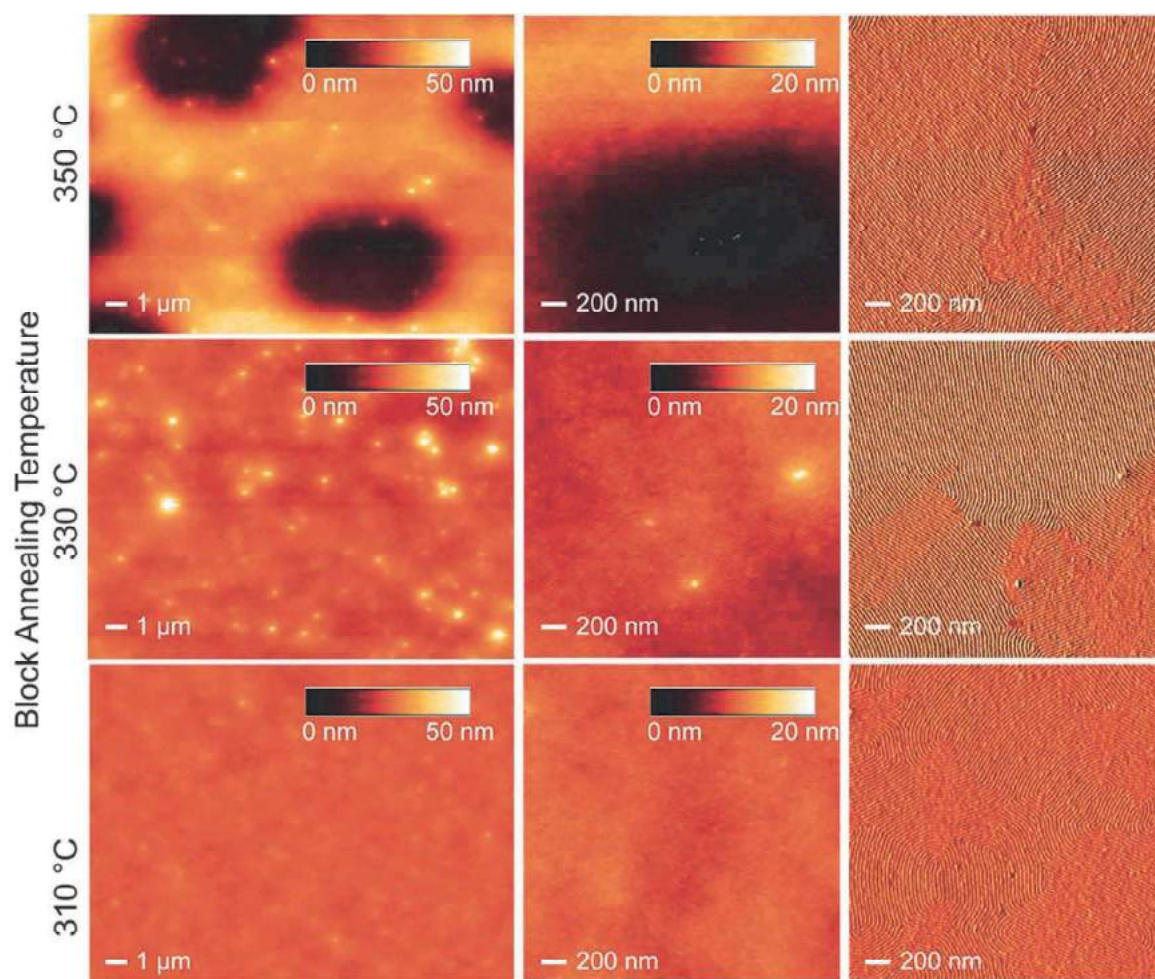


Figure 12. AFM analysis of B50 films annealed at different temperatures for 1 min after being spun on BrR58 treated at 330°C for 10 min. The heights of the topographic features and their sizes are coded according to the inset color tables and scale bars. The tapping-mode phase signal images corresponding to the areas in the central column are outlined in the right column.

The high-resolution AFM images in Figure 13 revealed that the point-like inhomogeneities are sharply-shaped points with height of about 20-30 nm on the surface of the film and form localized imperfections of the lamellar pattern, corresponding to an abrupt local variation in the number of lamellae. We can hypothesize that, during annealing, the BCP film undergoes some thermal expansion and the lamellae tend to lengthen. When a lamella interrupts, its local

1
2
3
4 expansion cannot be spread over the entire length of the lamella in order to accommodate the
5
6 elongated structure within the network. Consequently, the lamella bumps on top of other
7
8 lamellae, giving rise to a local ‘eruption’ of the polymeric film that expands above the layer and
9
10 cannot then relax back in the film upon the subsequent reduction of the temperature. As these
11
12 inhomogeneities derive from a variation in the number of lamellae converging on and diverging
13
14 from the defect point, their formation should be inhibited in topographically registered structures
15
16 where the number of lamellae is kept constant due to the external constraints imposed by the
17
18 prepatterned substrate.
19
20
21
22
23
24
25
26
27
28
29
30
31
32
33
34
35
36
37
38
39
40
41
42
43
44
45
46
47
48
49
50
51
52
53
54
55
56
57
58
59
60

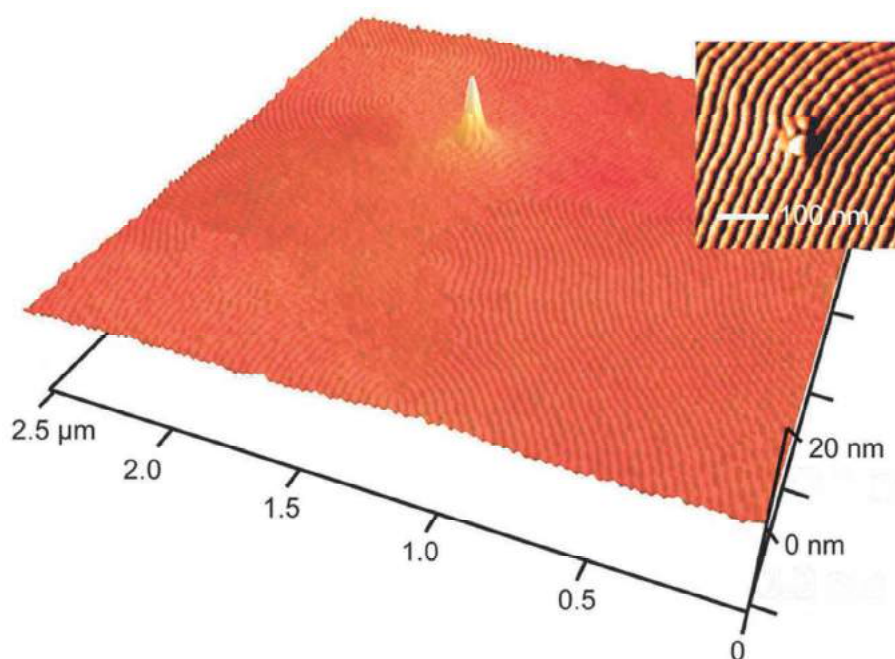


Figure 13. AFM perspective view of a detail of the surface of the B50 film annealed at 330°C for 1 min on BrR58 and showing a point-like inhomogeneity.

CONCLUSIONS

To increase the thermal stability of the random copolymer grafted layer, two converging strategies were described. From one side, a high temperature thermal treatment of a commercial

1
2
3 α -hydroxyl ω -TEMPO functional random copolymer TR58 leads to the formation of a stabilized
4 layer able to induce the perpendicular orientation of a homogeneous block copolymer thin film
5 up to temperatures as high as 310°C. On the other side, a α -hydroxyl ω -Br functional random
6 copolymer BrR58 with the same molar mass and composition of TR58, was prepared and
7 studied. The thermal stability of BrR58 was found inherently higher than TR58. In addition, once
8 subjected to high temperature thermal treatment, the thin copolymer layer deriving from BrR58
9 was demonstrated to be able to efficiently support the block copolymer ordering up to 330°C.
10 Comparison of the thermal analyses and the morphology data clearly reveals that the disruption
11 of the block copolymer layer, deposited on the grafted random copolymer layer, occurs because
12 of the formation of bubbles, due to a low temperature evolution of monomers from the random
13 copolymer layer. During their growth, these bubbles first start detaching the block copolymer
14 from the random layer and then break the block copolymer layer. Both TR58 and BrR58 share
15 the same behavior although the extent of the low temperature monomer evolution is higher for
16 the former sample and starts at lower temperatures. For both copolymers, the thermal treatment
17 offsets the low temperature monomer evolution while still maintaining surface characteristics
18 suitable to induce the perpendicular orientation of the block copolymers. As the grafting reaction
19 of the random copolymers to the silicon wafer can occur in parallel with the stabilizing thermal
20 treatment, this process does not represent an additional step in the processing workflow of the
21 block copolymers to obtain nanomanufactured surfaces. This process can be easily integrated
22 into a production line thus ultimately extending the range of processing temperatures of the block
23 copolymer film and consequently speeding up the self-organization process.
24
25
26
27
28
29
30
31
32
33
34
35
36
37
38
39
40
41
42
43
44
45
46
47
48
49
50
51
52
53
54
55
56
57
58
59
60

1
2
3 AUTHOR INFORMATION
45
6 **Corresponding Author**
78
9 * E-mail: michele.laus@mfu.unipmn.it, michele.perego@mdm.imm.cnr.it.
10
1112
13 **Author Contributions**
1415
16 The manuscript was written through contributions of all authors. All authors have given approval
17
18 to the final version of the manuscript.
1920
21
22 ACKNOWLEDGMENT
2324
25 This research activity was partially funded by the ERANET PLUS “NanoSci-E+” consortium
26
27 through the NANO-BLOCK project, and by the European Metrology Research Programme
28
29 (EMRP), project new01-TReND. The EMRP is jointly funded by the EMRP participating
30
31 countries within EURAMET and the European Union. Partial financial support by PRIN 2010-
32
33 2011 "Materiali Polimerici Nanostrutturati con Strutture Molecolari e Cristalline Mirate" is
34
35 acknowledged. Patent protection related to this work is pending.
36
37
3839
40 **Notes**41 The authors declare no competing financial interest.
42
43
4445
46 REFERENCES
47

- 48
-
- 49 (1) Li, M.; Ober, C. K. Block Copolymer Patterns and Templates.
- Mater. Today*
- 2006**
- ,
- 9*
- , 30–
-
- 50
-
- 51 39.
-
- 52
-
- 53
-
- 54 (2) Darling, S. B. Directing the Self-Assembly of Block Copolymers.
- Prog. Polym. Sci.*
-
- 55
-
- 56
- 2007**
- ,
- 32*
- , 1152–1204.
-
- 57
-
- 58
-
- 59
-
- 60

1
2
3 (3) Hamley, I. W. Ordering in Thin Films of Block Copolymers: Fundamentals to Potential
4 Applications. *Prog. Polym. Sci.* **2009**, *34*, 1161–1210.
5
6

7
8
9 (4) Kim, H. C.; Park, S. M.; Hinsberg, W. D. Block Copolymer Based Nanostructures:
10 Materials, Processes, and Applications to Electronics. *Chem. Rev.* **2010**, *110*, 146–177.
11
12

13
14 (5) Bates, C. M.; Maher, M. J.; Janes, D. W.; Ellison, C. J.; Willson, C. G. Block Copolymer
15 Lithography. *Macromolecules* **2014**, *47*, 2–12.
16
17

18
19 (6) Kim, S. O.; Solak, H. H.; Stoykovich, M. P.; Ferrier, N. J.; de Pablo, J. J.; Nealey, P. F.
20 Epitaxial Self-Assembly of Block Copolymers on Lithographically Defined Nanopatterned
21 Substrates. *Nature* **2003**, *424*, 411–414.
22
23
24

25
26 (7) Fasolka, M. J.; Banerjee, P.; Mayes, A. M.; Pickett, G.; Balazs, A. C. Morphology of
27 Ultrathin Supported Diblock Copolymer Films: Theory and Experiment. *Macromolecules* **2000**,
28 *33*, 5702–5712.
29
30
31
32

33
34 (8) Peters, R. D.; Yang, X. M.; Kim, T. K.; Sohn, B. H.; Nealey, P. F. Using Self-Assembled
35 Monolayers Exposed to X-Rays to Control the Wetting Behavior of Thin Films of Diblock
36 Copolymers. *Langmuir* **2000**, *16*, 4625–4631.
37
38
39
40

41
42 (9) Peters, R. D.; Yang, X. M.; Kim, T. K.; Nealey, P. F. Wetting Behavior of Block
43 Copolymers on Self-Assembled Films of Alkylchlorosiloxanes: Effect of Grafting Density.
44 *Langmuir* **2000**, *16*, 9620–9626.
45
46
47
48

49
50 (10) Borah, D.; Ozmen, M.; Rasappa, S.; Shaw, M. T.; Holmes, J. D.; Morris, M. Molecularly
51 Functionalized Silicon Substrates for Orientation Control of the Microphase Separation of PS-*b*-
52 PMMA and PS-*b*-PDMS Block Copolymer Systems. *Langmuir* **2013**, *29*, 2809–20.
53
54
55
56
57
58
59
60

1
2
3 (11) Mansky, P.; Liu, Y.; Huang, E.; Russell, T. P.; Hawker, C. Controlling Polymer-Surface
4 Interactions with Random Copolymer Brushes. *Science* **1997**, *275*, 1458–1460.
5
6

7
8 (12) Ryu, D. Y.; Shin, K.; Drockenmuller, E.; Hawker, C. J.; Russell, T. P. A Generalized
9 Approach to the Modification of Solid Surfaces. *Science* **2005**, *308*, 236–239.
10
11

12
13 (13) Shengxiang, J.; Liu, G.; Zheng, F.; Craig, G. S. W.; Himpsel, F. J.; Nealey, P. F.
14 Preparation of Neutral Wetting Brushes for Block Copolymer Films from Homopolymer Blends.
15
16
17
18
19
20
21
22

23 (14) Bates, C. M.; Strahan, J. R.; Santos, L. J.; Mueller, B. K.; Bamgbade, B. O.; Lee, J. a;
24 Katzenstein, J. M.; Ellison, C. J.; Willson, C. G. Polymeric Cross-Linked Surface Treatments for
25 Controlling Block Copolymer Orientation in Thin Films. *Langmuir* **2011**, *27*, 2000–2006.
26
27
28
29

30 (15) Jung, H.; Leibfarth, F. a.; Woo, S.; Lee, S.; Kang, M.; Moon, B.; Hawker, C. J.; Bang, J.
31 Efficient Surface Neutralization and Enhanced Substrate Adhesion through Ketene Mediated
32 Crosslinking and Functionalization. *Adv. Funct. Mater.* **2013**, *23*, 1597–1602.
33
34
35
36
37

38 (16) Bang, J.; Bae, J.; Löwenhielm, P.; Spiessberger, C.; Given-Beck, S. A.; Russell, T. P.;
39 Hawker, C. J. Facile Routes to Patterned Surface Neutralization Layers for Block Copolymer
40 Lithography. *Adv. Mater.* **2007**, *19*, 4552–4557.
41
42
43
44
45

46 (17) In, I.; La, Y.-H.; Park, S.-M.; Nealey, P. F.; Gopalan, P. Side-Chain-Grafted Random
47 Copolymer Brushes as Neutral Surfaces for Controlling the Orientation of Block Copolymer
48 Microdomains in Thin Films. *Langmuir* **2006**, *22*, 7855–60.
49
50
51
52

53 (18) Han, E.; Gopalan, P. Cross-Linked Random Copolymer Mats as Ultrathin
54 Nonpreferential Layers for Block Copolymer Self-Assembly. *Langmuir* **2010**, *26*, 1311–1315.
55
56
57
58
59
60

1
2
3 (19) Seguini, G.; Giammaria, T. J.; Ferrarese Lupi, F.; Sparnacci, K.; Antonioli, D.; Gianotti,
4 V.; Vita, F.; Placentino, I. F.; Hilhorst, J.; Ferrero, C.; Francescangeli, O.; Laus, M.; Perego, M.
5 Thermally Induced Self-Assembly of Cylindrical Nanodomains in Low Molecular Weight PS-b-
6 PMMA Thin Films. *Nanotechnology* **2014**, *25*, 045301.
7
8

9
10
11
12
13 (20) Ferrarese Lupi, F.; Giammaria, T. J.; Seguini, G.; Vita, F.; Francescangeli, O.; Sparnacci,
14 K.; Antonioli, D.; Gianotti, V.; Laus, M.; Perego, M. Fine Tuning of Lithographic Masks
15 through Thin Films of PS-b-PMMA with Different Molar Mass by Rapid Thermal Processing.
16 *ACS Appl. Mater. Interfaces* **2014**, *6*, 7180–7188.
17
18
19

20
21
22 (21) Ham, S.; Shin, C.; Kim, E.; Ryu, D. Y.; Jeong, U.; Russell, T. P.; Hawker, C. J.
23 Microdomain Orientation of PS- b -PMMA by Controlled Interfacial Interactions.
24 *Macromolecules* **2008**, *41*, 6431–6437.
25
26
27

28
29 (22) Han, E.; Stuen, K. O.; La, Y. H.; Nealey, P. F.; Gopalan, P. Effect of Composition of
30 Substrate-Modifying Random Copolymers on the Orientation of Symmetric and Asymmetric
31 Diblock Copolymer Domains. *Macromolecules* **2008**, *41*, 9090–9097.
32
33
34

35
36 (23) Han, E.; Stuen, K. O.; Leolukman, M.; Liu, C. C.; Nealey, P. F.; Gopalan, P.
37 Perpendicular Orientation of Domains in Cylinder-Forming Block Copolymer Thick Films by
38 Controlled Interfacial Interactions. *Macromolecules* **2009**, *42*, 4896–4901.
39
40
41

42
43 (24) Ballard, C. C.; Broge, E. C.; Iler, R. K.; St John, D. S.; McWhorter, J. R. Esterification of
44 the Surface of Amorphous Silica. *J. Phys. Chem.* **1961**, *65*, 20–25.
45
46
47

48
49 (25) Dion, M.; Rapp, M.; Rorrer, N.; Shin, D. H.; Martin, S. M.; Ducker, W. A. The
50 Formation of Hydrophobic Films on Silica with Alcohols. *Colloids Surf. A* **2010**, *362*, 65–70.
51
52
53

1
2
3 (26) Liu, C.-C.; Thode, C. J.; Rincon Delgadillo, P. A.; Craig, G. S. W.; Nealey, P. F.;
4
5 Gronheid, R. Towards an All-Track 300 mm Process for Directed Self-assembly. *J. Vac. Sci.*
6
7 *Technol., B: Microelectron. Process. Phenom.* **2011**, *29*, 06F203.

8
9
10
11 (27) Ferrarese Lupi, F.; Giammaria, T. J.; Seguini, G.; Ceresoli, M.; Perego, M.; Antonioli,
12
13 D.; Gianotti, V.; Sparnacci, K.; Laus, M. Flash Grafting of Functional Random Copolymers for
14
15 Surface Neutralization. *J. Mater. Chem. C* **2014**, *2*, 4909.

16
17
18 (28) Metwalli, E.; Perlich, J.; Wang, W.; Diethert, A.; Roth, S. V.; Papadakis, C. M.; Müller-
19
20 Buschbaum, P. Morphology of Semicrystalline Diblock Copolymer Thin Films upon Directional
21
22 Solvent Vapor Flow. *Macromol. Chem. Phys.* **2010**, *211*, 2102–2108.

23
24
25 (29) Sinturel, C.; Vayer, M.; Morris, M.; Hillmyer, M. Solvent Vapor Annealing of Block
26
27 Polymer Thin Films. *Macromolecules* **2013**, *46*, 5399–5415.

28
29
30 (30) Ferrarese Lupi, F.; Giammaria, T. J.; Ceresoli, M.; Seguini, G.; Sparnacci, K.; Antonioli,
31
32 D.; Gianotti, V.; Laus, M.; Perego, M. Rapid Thermal Processing of Self-Assembling Block
33
34 Copolymer Thin Films. *Nanotechnology* **2013**, *24*, 315601.

35
36
37 (31) Mansky, P.; Russell, T. P.; Hawker, C. J.; Mays, J.; Cook, D. C.; Satija, S. K. Interfacial
38
39 Segregation in Disordered Block Copolymers: Effect of Tunable Surface Potentials. *Phys. Rev.*
40
41 *Lett.* **1997**, *79*, 237–240.

42
43
44 (32) Welander, A. M.; Kang, H.; Stuen, K. O.; Solak, H. H.; Müller, M.; de Pablo, J. J.;
45
46 Nealey, P. F. Rapid Directed Assembly of Block Copolymer Films at Elevated Temperatures.
47
48 *Macromolecules* **2008**, *41*, 2759–2761.
49
50
51
52
53
54
55
56
57
58
59
60

1
2
3 (33) Perego, M.; Ferrarese Lupi, F.; Ceresoli, M.; Giammaria, T. J.; Seguini, G.; Enrico, E.;
4 Boarino, L.; Antonioli, D.; Gianotti, V.; Sparnacci, K.; Laus, M. Ordering Dynamics in
5 Symmetric PS-*b*-PMMA Diblock Copolymer Thin Films During Rapid Thermal Processing. *J.*
6 *Mater. Chem. C* **2014**, *2*, 6655–6664.
7
8

9
10
11
12
13 (34) Ceresoli, M.; Ferrarese Lupi, F.; Seguini, G.; Sparnacci, K.; Gianotti, V.; Antonioli, D.;
14 Laus, M.; Boarino, L.; Perego, M. Evolution of Lateral Ordering in Symmetric Block Copolymer
15 Thin Films upon Rapid Thermal Processing. *Nanotechnology* **2014**, *25*, 275601.
16
17
18

19
20
21 (35) Gianotti, V.; Antonioli, D.; Sparnacci, K.; Laus, M.; Giammaria, T. J.; Ferrarese Lupi, F.;
22 Seguini, G.; Perego, M. On the Thermal Stability of PS-*b*-PMMA Block and PS-*r*-PMMA
23 Random Copolymers for Nanopatterning Applications. *Macromolecules* **2013**, *46*, 8224–8234.
24
25
26

27
28
29 (36) Borah, D.; Rasappa, S.; Senthamarai kanna, R.; Shaw, M. T.; Holmes, J. D.; Morris, M.
30 The Sensitivity of Random Polymer Brush-Lamellar Polystyrene-*b*-Polymethylmethacrylate
31 Block Copolymer Systems to Process Conditions. *J. Colloid Interface Sci.* **2013**, *393*, 192–202.
32
33
34

35
36
37 (37) The International Technology Roadmap for Semiconductors (ITRS), “Emerging
38 Research Materials” **2007**.
39
40

41
42
43 (38) Koo, K.; Ahn, H.; Kim, S.-W.; Ryu, D. Y.; Russell, T. P. Directed Self-Assembly of
44 Block Copolymers in the Extreme: Guiding Microdomains from the Small to the Large. *Soft*
45 *Matter* **2013**, *9*, 9059–9071.
46
47
48

49
50
51 (39) Jakubowski, W.; Min, K.; Matyjaszewski, K. Activators Regenerated by Electron
52 Transfer for Atom Transfer Radical Polymerization of Styrene. *Macromolecules* **2006**, *39*, 39–
53 45.
54
55
56
57
58
59
60

1
2
3
4 (40) Granel, C.; Dubois, P.; Jérôme, R.; Teyssié, P. Controlled Radical Polymerization of
5
6 Methacrylic Monomers in the Presence of a Bis (ortho-chelated) Arylnickel (II) Complex and
7
8 Different Activated Alkyl Halides. *Macromolecules* **1996**, *29*, 8576–8582.
9

10
11 (41) Moineau, G.; Minet, M.; Dubois, P.; Teyssie, P.; Senninger, T.; Jerome, R. Controlled
12
13 Radical Polymerization of (Meth)acrylates by ATRP with $\text{NiBr}_2(\text{PPh}_3)_2$ as Catalyst.
14
15 *Macromolecules* **1999**, *32*, 27–35.
16
17

18
19 (42) Colombani, D.; Steenbock, M.; Klapper, M.; Mullen, K. 1,3,5,5-Tetraphenyl-D3-1,2,4-
20
21 triazolin-2-yl Radical-Properties in the Controlled Radical Polymerization of Poly(methyl
22
23 methacrylate) and Polystyrene. *Macromol. Rapid Commun* **1997**, *18*, 243–251.
24
25

26
27 (43) Lehrle, R.; Shortland, A. Reproducibility of Filament Pyrolysers: Influence of Sample
28
29 Deposition and Other Factors *Eur. Polym. J.* **1993**, *29*, 1277–1282.
30
31

32
33 (44) Lehrle, R.; Atkinson, D. J.; Bate, D.; Gardner, P.; Grimbley, M.; Groves, S.; Place, E.;
34
35 Williams, R. Diagnosis Mechanisms of Oligomers Formation in the Thermal Degradation of
36
37 Polymers. *Polym. Degrad. Stab.* **1996**, *52*, 183–196.
38
39

40
41 (45) Manring, L. E. Thermal Degradation of Poly(methyl methacrylate)2. Vinyl-Terminated
42
43 Polymer. *Macromolecules* **1989**, *22*, 2673–2677.
44
45

46
47 (46) Gianotti, V.; Antonioli, D.; Sparnacci, K.; Laus, M.; Giammaria, T. J.; Ceresoli, M.;
48
49 Ferrarese Lupi, F.; Seguini, G.; Perego, M. Characterization of Ultra-Thin Polymeric Films by
50
51 Gas Chromatography-Mass Spectrometry Hyphenated to Thermogravimetry. *J. Chromatogr. A*
52
53 **2014**, *1368*, 204–210.
54
55
56
57
58
59
60

1
2
3 (47) Russell, T. P.; Hjelm, R. P.; Seeger, P. A. Temperature Dependence of the Interaction
4
5
6 Parameter of Polystyrene and Poly (methyl methacrylate). *Macromolecules* **1990**, *23*, 890–893.
7
8
9
10
11
12
13
14
15
16
17
18
19
20
21
22
23
24
25
26
27
28
29
30
31
32
33
34
35
36
37
38
39
40
41
42
43
44
45
46
47
48
49
50
51
52
53
54
55
56
57
58
59
60